3-D seismic analysis using remote sensing techniques

Richard J. Pegoraro and Robert R. Stewart

ABSTRACT

Techniques for the processing and interpretation of remotely sensed data have been widely used for various applications relating to surface and near surface environments (especially forest, crops, surface geological features, and oceans). This study applies these same techniques in an attempt to classify and quantify features which are subsurface in nature and have been gathered by current seismic techniques, and to see if the geology is evident in the texture of the seismic reflections. These techniques produce a series of images at various depths based on the reflections of the signals by the different rock layers. The strength of these reflections (their brightness values) can then be processed much in the same way as airborne radar type data, giving a more clear picture to interpreters with respect to the subsurface features. This study found that the selected features could be separated by the classifier very well with an average accuracy of 95% or greater for all feature classes with the training sites selected. The results for the test sites also achieved accuracy values of 85% or higher for the three test classifications. The separability of the signatures for the test and training sites were also found to be 1.99 or higher in average which is very good, the maximum separability being 2.0.

STUDY AREA

The data in this study is from a standard 3-D seismic volume generated in the Cold Lake region of Alberta by Imperial Oil Resources Ltd. The specific location is in Township 65 Range 4, and covers a producing pad at Cold Lake which includes twelve injection/production wells. Imperial Oil is producing bitumen from the Clearwater sands via an enhanced oil recovery program. This procedure uses steam injection at high temperature and pressure to lower viscosity and allow for recovery. One seismic survey was acquired in 1990 during a production cycle, and the second was taken in 1992 during an injection cycle. The oil sands are contained within the Mannville group, which contain the primary reservoir of the Clearwater formation. This formation is a transgressive wedge with the sands being primarily deltaic and foreshore/shoreface facies. These sands are highly saturated with a low specific gravity and high viscosity bitumen. The specific gravity of the bitumen is of the order of 10 gm/cc and is free of underlying water (Isaac and Lawton, 1993)

Conditions prevalent during the injection process, high temperatures and pressure, caused a decrease in compressional wave velocity. The result of this decrease is the time structures below the reservoir on the 1992 survey are later than those on the 1990 survey. The effect has not been homogeneous across the pad but varies because of steam communication within the reservoir. Where the 1992 times are seen as "delayed" it can be said that the reservoir has been steamed.

The data consisted of a series of time slices removed from the 3-D seismic volume which included the Devonian time structure, which was the one used for this initial study. This image is below the reservoir and as such, will be affected by the presence of steam shallower. The depth of the Devonian time structure image is approximately 560 meters below the surface (Isaac and Lawton, 1994).

METHODS

The seismic images provided by the 3-D seismic data were down loaded to a 3.5 floppy disk in a Tiff format complete with associated pseudo color table. These images were loaded in a compressed format which was not readable to the Easi/Pace system and which required translation on a Mac computer. The Mac system was able to read the data, and the information was then translated to Jpeg format and transferred to the disk in and uncompressed Tiff format from the Jpeg, which was then readable to the Easi/Pace system. The images were read into a PCI data base using the tiffread module which automatically converts the data to a PCI data base format. The images which were of slightly different sizes, but were automatically scaled to fit a 512 by 512 pixel size data base format with a pixel size of 1 meter by 1 meter. These images were then processed in the same way one would process satellite type surface data for classification and enhancement purposes. This was accomplished by using the several types of filters, both standard and programmable, which are contained in the Easi/Pace package. The main filters used were the mean, median, and mode which gave the best results in smoothing the data and removed noise and confusion, while at the same time preserving the detail contained in the image. Several other types of filters were also employed in an effort to clarify the structural components contained within the image. These included edge enhancements, and the Frost adaptive filter type as well as various high and low pass filters. This was done in an attempt to determine whether the filtering was able to provide any additional clearer information not available on the original image.

Once the images had been filtered, the Easi/Pace texture analysis package was employed to process the images for various types of texture. Within the package itself, there are five types of texture which can be applied to an image and these five were the primary ones used in the study.

TEXTURE MEASURES

The texture algorithms used were the standard ones available in the PCI image analysis system, which use the gray level co-occurrence matrix for calculation. The texture measures available in the package are;

1) Homogeneity : $\sum_{j=1}^{n}\sum_{i=1}^{m}\left(P_{i,j} \,/\, \left(1-\left(IR_i - IC_j\right)**2\right)\right)$

2) Contrast : $\sum_{i=1}^{m}\sum_{j=1}^{n}\left(P_{i,j} * \left(\left(IR_i - IC_j\right)**2\right)\right)$

3) Dissimilarity : $\sum_{i=1}^{m}\sum_{j=1}^{n}\left(P_{i,j} * \left|\left(IR_i - IC_j\right)\right|\right)$

4) Mean : $\sum_{i=1}^{m}\sum_{j=1}^{n}\left(IR_i * P_{i,j}\right)$

5) Standard Deviation : $\sqrt{\sum_{i=1}^{m}\sum_{j=1}^{n}\left(\left(P_{i,j} * IR_i - \text{mean}\right)**2\right)}$

6) Entropy : $-\left(\sum_{i=1}^{m}\sum_{j=1}^{n}\left(P_{i,j} * \mathrm{LOGe}\left(P_{i,j}\right)\right)\right), \mathrm{if}\left(P_{i,j} \langle\rangle 0\right)$

where :

$\Sigma(j=1,n)$: sum of the co-occurrence matrix elements (row).

$\Sigma(i=1,n)$: sum of the co-occurrence matrix elements (column).

P(i,j) : is a co-occurrence matrix element.

IR(i) : is the gray level for a row (i.e., reference).

IC(j) : is the gray level for a column (i.e., neighbor).

The texture measures of homogeneity, contrast, and entropy relate to specific textural characteristics of the image. The texture measures of mean, standard deviation, and dissimilarity characterize the complexity and nature of the gray level transitions which occur in the image (PCI, 1991). These measures are derived from the gray level co-occurrence matrix. The co-ocurrence matrix shows the relationship between a given pixel and its specified neighbor. Texture is related to the distance between the co-occurrence matrix elements and the diagonal elements of the matrix. The amount of dispersion that the matrix elements have about the diagonal may be measured statistically through the different texture measures. For example, the texture measure Contrast gives a non linearly increasing weight to the gray level transitions from a low gray scale value to a high gray scale value. This is the moment of inertia around the main diagonal of the matrix and measures the degree of spread of the matrix values. Entropy measures the number of gray level transitions from one gray level to another and gives a high value when the elements are equal or nearly equal and a low value when the elements are unequal. The texture measure Homogeneity measures the degree to which the rows and the columns of the matrix resemble each other. The values here are high when they are uniformly distributed in the matrix and are low otherwise (Haralick, 1975, Weszka et al., 1974). The standard deviation texture algorithm uses the average gray level value for the window and is given by the sum of the gray level values divided by one less than the number of elements in the window (i.e., n-1 elements). The algorithm then subtracts this value from the pixel gray level value at location (i,j) and squares the result. The sum of all elements in the window is then taken and divided by the number of elements in the window. The square root of this value is taken and this forms the standard deviation texture value of the center pixel in the window (Pegoraro, 1994).

IMAGE CLASSIFICATION

Once the various types of processed images were complete, training sites were extracted using the classification package of the system. This entailed the use of single pixel training site for purity and to reduce confusion between the selected classes. Using the original unprocessed image to select the training and testing sites, a set of seven distinct gray levels were identified and used to classify the image. These were selected using the display control package (DCP) to designate the training and testing sites, then using the signature generator module (CSG) to generate the signatures used

in the classification process. Several sets of signatures were used employing not only the original image, but also image data produced using the filters and the texture images generated. Up to eight layers were combined for the classification which produced the thematic map. The classification process used the full maximum likelihood classification algorithm from the classification module of the Easi pace program. This was the most accurate type available with this package.

The maximum likelihood classification algorithm provided in the program uses the Mahalanobis minimum distance algorithm (Hsu, 1979). This maximum likelihood classifier can be regarded as a minimum distance-like classifier but with a distance measure which is direction sensitive and modified according to class. The Mahalanobis distance is used to identify deviant members of the sample. Robust estimates of the mean and variance - covariance matrices are computed using weights which are functions of the distance. The effect is to downgrade the pixel values with a high Mahalanobis distance. These are the ones which are relatively far from the mean of the training class, taking into account the shape of the probability distribution of the training class members. The advantage of using the Mahalanobis classifier is that it is faster than the standard maximum likelihood classifiers but still retains a degree of direction sensitivity via the covariance matrix. The Mahalanobis distance used in the PCI system is defined by the following equation:

$$Gi(X) = -1/2(X-Ui)^t Ci^{-1}(X-Ui) - d/2\log(2\pi) - 1/2\log(\det(Ci)) + \log(Pi)$$

where:

Gi(X) : is the result for class i on pixel x

d : is the number of channels in the classification

X=(x1,..,xd) : is the (d by 1) pixel vector of gray levels

Ui : is the (d by 1) mean vector for class i

Ci : is the (d by d) covariance matrix for class i

π : is pi= 3.14159....

det(Ci) : is the determinant of the covariance matrix

t : as a superscript denotes transpose

-1 : as a superscript denotes inverse

Ti : is the threshold value THRS for class i

Pi=Bi/$\sum$(Bi) : is the apriori probability for class i

Bi : is the BIAS for class i

$\sum$(Bi) : is the sum of biases for all classes used

(d, Ui, Bi, Ti, |Ci|, Ci^{-1} ; are obtained from the signature segments)

The full maximum likelihood classifier uses a Gaussian threshold to determine if the pixel falls within the class or not. The decision rule assigns each pixel having features X to class i whose units are most probable or likely to have given rise to feature vector i. The classifier assumes the training data statistics for each class have a normal or Gaussian distribution in nature. The threshold is the radius in standard deviation units of a hyper ellipsoid surrounding the mean of the class in feature space. If the pixel falls inside the hyper ellipsoid, it is assigned to the class. This feature can be set by the operator. For the purpose of this study, the threshold for each classification was set at 16. This value was chosen after an initial trial run classification in order to reduce the number of unclassified pixels in the image to under 5%. The class bias is used to resolve the overlap between class (PCI, 1988). The bias for each class can also be set by the operator and gives a weight to the decision as to where the pixel will be classified. The default value of the bias is 1.00 and this value was left unchanged for the entire set of classifications, thus equal weighting for all classes. The confusion matrix for each classification is presented in the following set of tables:

class	cl 1	cl 2	cl 3	cl 4	cl 5	cl 6	cl 7
cl 1	96.5	3.5	-	-	-	-	-
cl 2	0.2	96.4	2.9	-	-	-	-
cl 3	-	1.3	98.7	-	-	-	-
cl 4	-	-	-	98.3	-	-	1.7
cl 5	-	-	-	-	99.0	-	1.0
cl 6	-	-	-	-	0.6	99.1	0.3
cl 7	-	-	-	-	-	-	99.9

Table 1 : Class accuracy for classification 2 (contrast texture).

class	cl 1	cl 2	cl 3	cl 4	cl 5	cl 6	cl 7
cl 1	97.8	1.9	-	-	-	-	-
cl 2	0.2	96.9	2.6	-	-	-	-
cl 3	-	2.1	97.9	-	-	-	-
cl 4	-	-	-	98.6	-	-	1.4
cl 5	-	-	-	-	99.0	-	0.7
cl 6	-	-	-	-	0.6	99.1	0.3
cl 7	-	-	-	-	-	-	99.7

Table 2 : Class accuracy for classification 3 (contrast/Dissimilarity with mode and edge detection filters).

The values given in the main diagonal of the confusion matrix presented in tables one and two reflect the accuracy values for each particular class. For class 1, the average class accuracy is 98.87% of the pixels correctly classified. The high value for the class is 100% with the lowest values being 94.3 % in the classifications which combined the signatures into other classes. Class 2 had an overall average accuracy of 92.41% over the eight classifications performed with a low value of 78.3 % (Dissimilarity, Standard Deviation, and Contrast texture combined) and a high value of 99.7% (Dissimilarity, Standard Deviation, and Contrast with 8 channel of data input). The areas of overlap was with classes 3 and 1, with the largest overlap being with class 3 (21.5%). Class 3 had an average value of 97.0% correctly classified over all classification schemes. Class 4 had an average accuracy of 98.55% over the six classification schemes using this class. Class 4's major area of overlap was with class 7 being as low as 0.0% with classification scheme 5 (Mean) and as high as 2.5% with classification scheme 6 (Contrast, Standard Deviation, Dissimilarity). Class 5 showed the least sensitivity to various combinations of texture or of only one texture measure being used for the classification. The minimum value achieved with this class was 95.1% with classification 7 and the best was 100% with classification 5. Class 5 also had overlap with class 7 (2.6%) and with class 3 (2.4%), but generally was very good. Class 6 achieved an average accuracy of 99.25% over all classification schemes and showed little sensitivity to the various combinations of texture or whether they were used singly. Class 6 also achieved the highest overall accuracy of any of the classes, and showed only minor overlap with classes 5 and 7 being less than 1% in all cases. Class 7 achieved an average accuracy of 97.36%, and showed only very little confusion with other classes. The following figure compares the relative accuracy of the various classification schemes using different texture measures both in combination and alone. Series 1 used dissimilarity texture (3 X 3 window) in addition to four channels of data for signature generation. Series 2 used contrast texture with a 5 X 5 window as well as four other channels of data. Series 3 used eight channels of information to generate the signatures used. These included two texture images, both dissimilarity and homogeneity texture measures. Series 4 used only three input

channels of information to generate the signatures, one of these being contrast texture. Series 6 used eight channels to generate the signatures with four being texture images. These four were contrast , standard deviation, dissimilarity , and homogeneity.

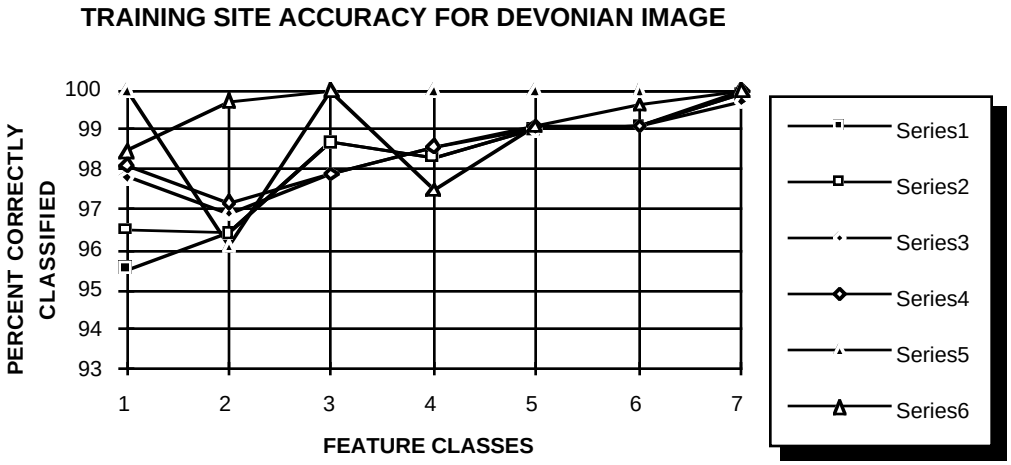

Figure 1 : Training site accuracy comparison.

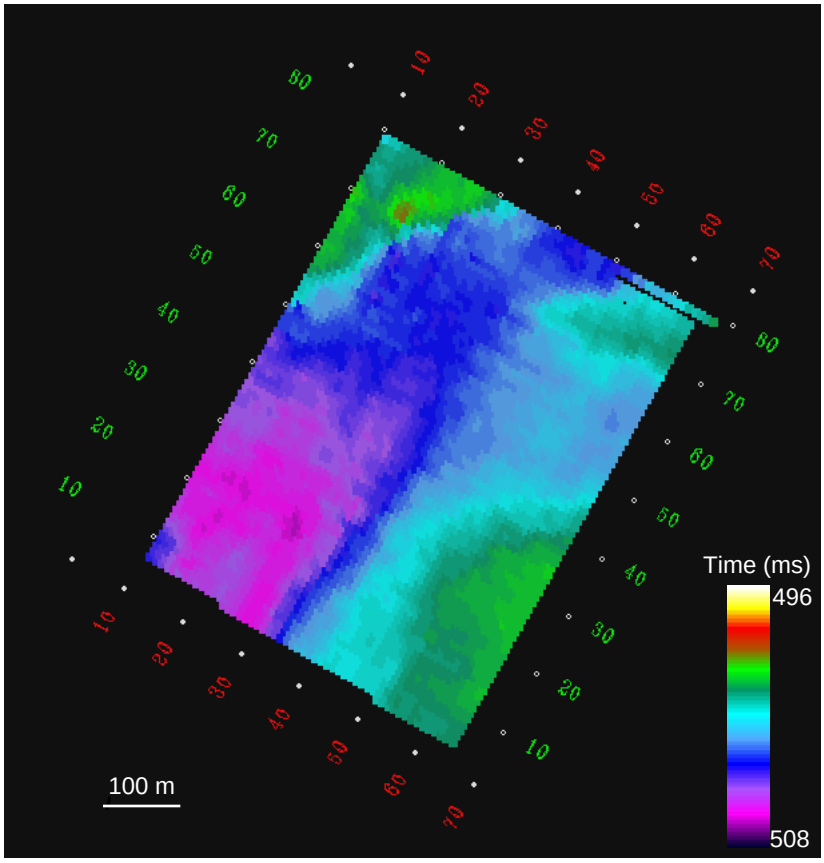

Figure 2: Original 3D image of Devonian time structure.

The image shown in figure 2 is the original time structure map used in the study. The pseudo coloring of the image indicates the time delay of the signal according to the scale located in the lower right hand corner. The scale located in the lower left indicates the size of the image in meters.

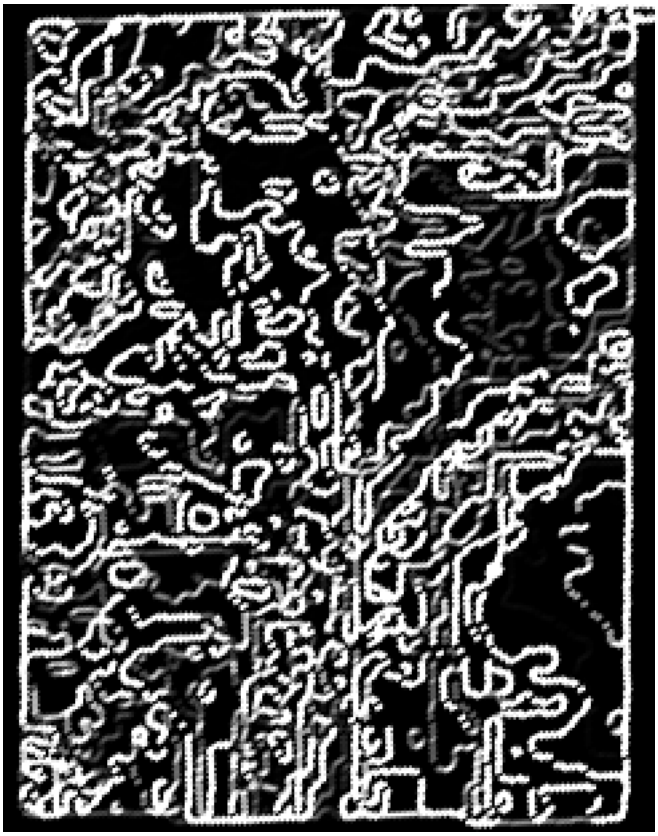

Figure 3: Image processes for contrast texture (3 X 3 filter size).

The image produced in figure 3 relates specifically to the textural characteristics of the original 3-D image presented in figure 2. The contrast texture measure gives a non linearly increasing weight to the gray level transitions as the window is moved across the image. These gray level transitions relate to the time delay of the signal return as it is presented in the original data. As the window is moved across the image, a value is calculated for the contrast texture for that region and is assigned to the center pixel within the window, in this case a 3 X 3 window size. The greater the rate of change from one pixel to the next in the window, the greater the weight that is assigned to the calculation, and thus the higher the pixel value assigned. This results in the high pixel values seen at the areas of greatest transition between one time delay value and the next. Areas where the transition in the brightness values (which relate directly to the time delay) was relatively low, the assigned pixel values are also low resulting in the darker gray and black areas in the image. From the spatial distribution of the pattern in figure 3, a visual display of the rate of change of the time delay values is presented, with greater rates of change being where the lines are more closely spaced.

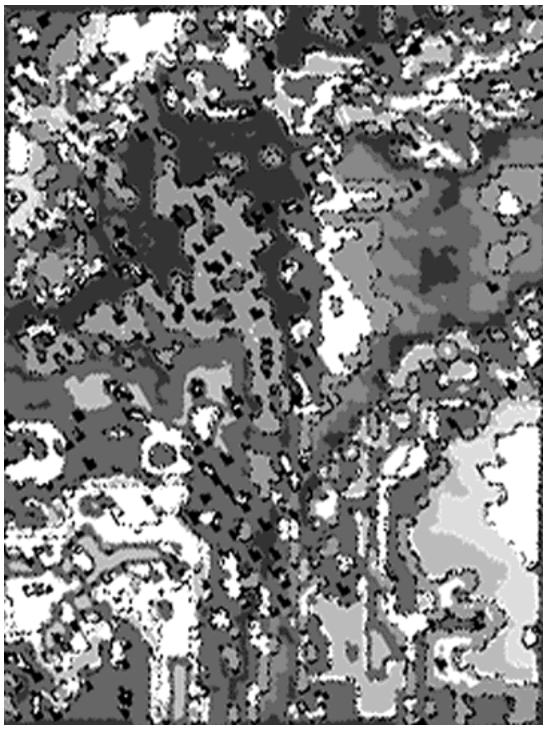

Figure 4: Classification 3 theme map using contrast and dissimilarity texture images.

The thematic maps produced show the results of the classification process. The thematic map shown in figure 4 is the result of the maximum likelihood classifier using signatures which included both contrast and dissimilarity texture measures as well as standard filtered images and the unfiltered data. This image corresponds to the accuracy values given in table 3 listed previously.

The data presented on the thematic map produced by the classification process shows an overall apparent increase in the detail presented when compared to the original image. The time structure presented in the image dips relatively smoothly from the upper right corner to the lower left and from right to left., and there are no outstanding or distinct anomalies or features present in the image. There is a high area also located in the upper right hand corner of the image as well as in the lower left. The themeatic map represents the slope as a series of steps in gray level in much the same way that a contour map represents changes in surface elevations. The time delay values are related directly to the gray levels of each step. The classification process breaks the data into distinct classes rather than the more general shaded appearance of the original data. The theme map shows the area in the lower left corner as being assigned the same class as the higher area in the upper and lower right corners. This is a result of how the original image was downloaded. The image assigned similar gray levels to both areas and then the image was pseudo colored to reflect the difference in time delay by the operator with the colors reflecting the time structure. When the maximum likelihood algorithm processed the image, the similarity of the gray levels in the samples result in the lower left area being coded the same as the areas in the lower right and upper left hand corners.

The image produced by the contrast texture algorithm quantifies the changes in gray level in the original image by giving a nonlinear increasing weight to changes in the

gray levels from low to high. This algorithm produces an image which appears much like a edge enhancement but with different levels of gray depending upon the change of gray level from one pixel to the next. The bright lines or edges correspond to changes in brightness values, with the greatest variations in the time delay over distance being the brightest and the smallest changes being dark areas. The image displayed in figure 3 formed one of the eight layers of image data which also included the original unprocessed data as well as filtered information which were combined to sample for the creation of the signature segments used in the classification process.

The classifications accuracy was confirmed by creation of test sites which were seen as representative of the various classes. These sites were selected as representative of the various feature but were of approximately five by five pixels in size. The sites were chosen in different areas from the original training sites. The classification process was repeated using the same technique as the first series of classifications. The results of the classifications using the test sites are presented in the following tables.

class	cl 1	cl 2	cl 3	cl 4	cl 5	cl 6	cl 7
cl 1	96.7	3.3	-	-	-	-	-
cl 2	-	100	-	-	-	-	-
cl 3	-	5.1	94.9	-	-	-	-
cl 4	-	-	-	100	-	-	-
cl 5	-	-	-	-	93.9	6.1	-
cl 6	-	0.4	-	-	-	99.6	-
cl 7	-	0.4	-	-	-	-	99.6

Table 3: Test 3 accuracy (Contrast / Dissimilarity texture).

As can be seen from table 3 , the accuracy of classes 2, 4, 6, and 7 are very good. The values for these classes are 99% or higher being correctly classified. The lowest value of class accuracy is with the first class when the three texture measures were used. This is also apparent for class 3 which showed a 10% drop in accuracy from the other test classifications using only two texture measures. Class 5, however, showed an equal accuracy when either the two or three texture measures were used (95.1%). When these results are compared to the ones achieved in the original series of classifications it can be seen that there are small differences in the overall accuracy values, depending upon which texture measures were used and how many were used. Also, the number of layers of information used in the classification was noticed to have an effect on the overall accuracy of the classifications. The following figure compares the relative accuracy of classifications of the three test classifications. Series 1 used contrast with standard deviation and dissimilarity texture measures in the layers of data samples for the signatures. Series 2 used only contrast and dissimilarity texture measures. Series three used the same texture measures as series 2, but used different

additional layers of data processed with different filters and window sizes.

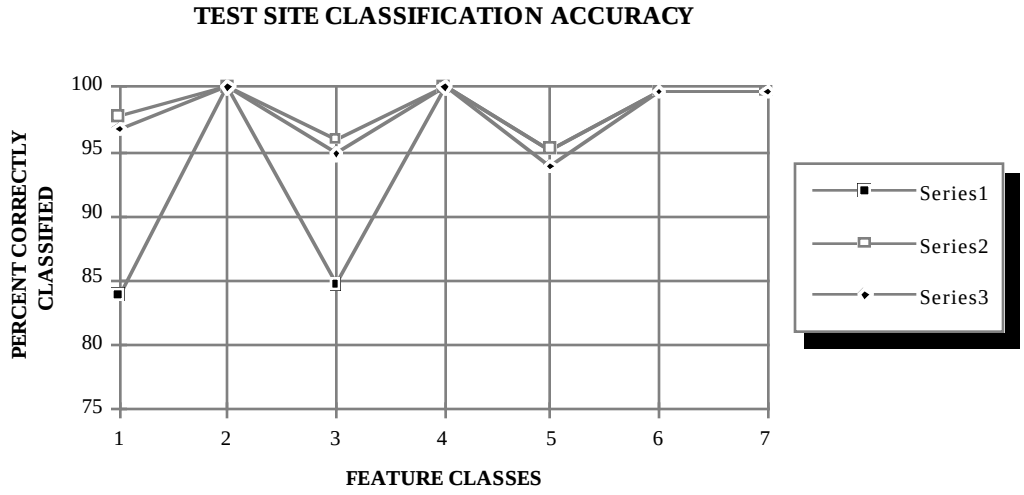

Figure 5: Test site accuracy comparison.

SIGNATURE SEPARABILITY

The signatures were the statistically tested using the Bhattacharrya distance to measure signature separability and the CSR feature of Easi/Pace package was used to generate statistics of each signature to check for any anomalies or problems. The Bhattacharya Distance equation assigns real values between 0.0 and 2.0 as a signature separability measure convention, and assumes the two classes being investigated are Gaussian in the nature of their distributions and uses the means and covariance matrices in the calculation. A value of 0.0 indicates complete overlap between the signatures, where as a value of 2.0 would indicate no overlap whatsoever (complete separability). A separability value of 1.7 or higher is considered to be good, while a value of 1.9 or higher is considered to be very good. The Bhattacharyya Distance is given by the following equation:

$$BD\ (I,J) = 2 * [\ 1\text{-}EXP\ (-A(I,J))]$$

where :

BD (i,j) : is the Battacharyya Distance between class i and j.

$$a(i,j) = 0.125\left[M(i) - M(j)\right]^{t}\left[A(i,j)(M(i) - M(j))\right]^{-1} +$$

$$0.5\,Ln\left[\det(A(i,j)) / SQRT\left(\det(S(I) * \det(S(j))\right)\right]$$

t : as a superscript denotes transpose of a matrix.

M(i) : mean vector of class i; vector has N channel elements.

N channel = number of channels used)

S(i) : covariance matrix for class i which has N channel elements.

-1 : as a superscript denotes inverse of a matrix.

A(i,j) : 0.5*[S(i) + S(j)].

S(i) : covariance matrix for class i which has N channel elements.

det ( ) : the determinant of a matrix.

Ln [ ] : the natural logarithm of a scalar value.

SQRT : the square root of a scalar value.

The values obtained for the signature separability for the signatures used in the classifications are given in the following table;

SEP MEAS.	MAXIMUM	MINIMUM	AVERAGE	DATA (TEX)
BD	2.0	1.999	1.999	Dissimilarity
BD	2.0	1.988	1.999	Contrast
BD	2.0	1.907	1.995	Dis/Homog
BD	2.0	1.908	1.995	Dis/ Homog
BD	2.0	1.768	1.988	Mean
BD	2.0	1.953	1.997	Con/Std/Dis

Table 4 : Signature separability values (Bhattacharrya) for the classifications.

It can be seen that the values for the average signature separability are above 1.9 for all classifications. These classifications not only used several texture images but also different filter sizes to process the image prior to running a classification Several classifications were run to see if there would be an improvement in the accuracy's by combining class signatures which appeared very similar. This was not the case, however, as the overall accuracy decreased and there was an increase in the amount of confusion between the various classes. It was also noted that classification schemes using multiple texture images as well as the original data and filtered data resulted in a slight reduction of signature separability when compared to classification schemes using only one texture image channel and filtered information. This could indicate increased confusion between the signatures due to overlap caused by the use of various filters and texture measures.

SEP MEAS.	MAXIMUM	MINIMUM	AVERAGE	DATA (TEX)
BD	2.0	1.999	1.999	D/CN/SD/M
BD	2.0	1.981	1.998	Dis/Mean
BD	2.0	1.985	1.998	Dis/Homog

Table 5 : Signature separability values (Bhattacharrya) for the three test sites.

As can be seen in table 5, the signature separability values of the test sites are comparable to the training sites. The values here are all 1.99 average or higher which means the separability of the signatures used for each class is very good for these particular test sites, and should have given clear and distinct signature samples for each class.

RESULTS

The use of texture and other contextual type of information has been used in the remote sensing community to increase the useful yield of data from a given set of images. This was done in an attempt to increase the accuracy of the thematic maps produced. The application of this type of methodology to the 3-D seismic volume processing is an attempt to process this information in a way that allows the multi-layering of data types to be used in order to generate signatures which would quantify features or characteristics of interest. This study used a data set produced from a standard seismic package, which produced a time structure image of the Devonian layer of the reservoir. This data was processed in the same way as a surface image would be and theme maps produced which represent features which were identified by the brightness value of the returned signal. The class accuracy values reported by the maximum likelihood report statistics package and also by the signature separability statistical package of the Easi/Pace system. These show that based on the reflectance values, features may be identified by the strength return of that particular feature, much like the reflectance values of surface features when viewed by Landsat satellites. The average accuracy's for the seven classes of reflectance values was between 92.41% (for class 2) and 100% (for class 5). These values indicate that it is possible to obtain clear or relatively clear signature values and therefore class accuracy’s from subsurface features in which the time delay values are spatially depicted via the image.

The potential problem exists, however, that because of the nature of the data and the resulting image, the separabilty may be a problematic due to the fact that the medium is relatively homogenous in nature. If the time structure or features being imaged is quite smooth, as it is in this case, the separation of the reflectance values may be difficult. This potential problem did not seem to be a factor in this study as the separability values between each class signature achieved were very good, the average values being between 1.98 and 1.99 for all classification schemes. This may be attributed to the single pixel sampling strategy which allows for very pure sample sites and therefore very clear and distinct signature gray levels with a great reduction in the amount of interclass confusion. These accuracy values were repeated for the test sites. Using the various combinations of texture and standard filtered images, accuracy values of 94% or higher in all cases except for class 1 and 2 in the first test classification were achieved. There was about a 10% accuracy reduction for these two classes and may be a result of the inclusion of the standard deviation texture image data. The texture algorithms when used in the classifications allowed for an improvement in classification

accuracy due to the ability to increase the separability of the signatures. However, in some cases, the use of multiple texture images in the creation of the signatures actually decreased the accuracy of specific classes, and as a result, the overall accuracy of the classification. This problem may have been in the texture algorithm chosen and how it quantifies the image data resulting in additional confusion being created rather than eliminated. A careful selection of the texture measures used would be necessary to ensure the most useful information and least amount of confusion for the classification. This reduction in accuracy may also be a result of the inclusion of filtered image data which blurred or created indistinct regions which were sampled for the creation of the signatures for those particular classes. A careful selection of the appropriate window size for filtering may reduce this type of confusion due to the fact that selection of a large window such as 11 X 11 may actually decrease the accuracy of the resulting classification. There is also the risk that the use of a small window size would also introduce noise and possible confusion. Optimum window size selection is as problematic here as it is in traditional remote sensing applications.

This initial study was conducted to investigate the possibility of using a remote sensing package to process seismic data in an effort to see if the image handling methods are able to present additional information beyond what is available in standard seismic data processing packages. The image of the time structure used in this study did not effectively connect the features presented with the gray level values in the image. The result of this was the assigned gray levels of both the lower right and left regions of the time structure image were the same and resulted in confusion in the classification. Such a connection would be required for the process to be truly effective in providing additional useful information. Despite the problems encountered in the classification process, the technique shows promise in its ability to separate and quantify features in the image by assigned gray levels. Further research into using this type of package for processing seismic data may show the ability to connect a specific reflectance value to a specific feature which would allow for the automation of classification and interpretation processes to an extent, as well as allowing the use of multiple layers of information upon which to base an interpretation. The images used for this initial study were based on hue and saturation and pseudo colored to reflect the nature of the time structure, and provided a starting point for this exploration. By changing the input images to ones which tie structure more directly to the gray level values presented in the image, it should be possible to identify specific features relatively accurately using the multiple layers of information and to increase the usefulness of the data presented.

REFERENCES

Gurney, C.M., 1987, *Texture Feature Extraction* : Pattern Recognition, Letters 6, 269-273

Haralick, R. M., 1975, *A Resolution Preserving Transform for Images* : Proceedings of the Conference on Computer Group; PR and Data Structure, May 14 - 16, 51 - 61.

Haralick, R. M., 1987, *Texture Feature Extraction* : Pattern Recognition Letters, 6, pp. 269 - 273.

Hsu, S.Y., 1978, *Texture - Tone Analysis for Automated Land Use Mapping* : PE & RS , 44, 1393 - 1404.

Hsu, S.Y., 1979, *The Mahalonobis Classifier with the Generalized Inverse Approach for Automated Analysis of Imagery Texture Data* : Academic Press Inc., GCIP-9, 117-134.

Hus, S.Y. and Burright, R., 1980, *Texture Perception and the RADC / Hsu Texture Feature Extractor* :

PE & RS, 46, 1051 - 1058.

Isaac, J.H. and Stewart, R.R., 1993, *3-D Seismic Expression of a Cryptoexplosion Structure* : Canadian Journal of Exploration Geophysics, 29, 429 - 439.

Isaac, J.H. and Lawton, D.C., 1994, *3-D and 3-C seismic data analysis at Cold Lake*, Alberta : Crewes Research Report, 6, 18.

Isaac, J.H. and Lawton, D.C., 1993, Cold Lake 3-D Seismic Analysis : Crewes Research Report, 5, 25-1- 25-16.

Mitchell, O.R., Meyers, C.R., and Boyne, W., 1977, *A Min-Max Measure for Image Texture Analysis* : IEEE Transactions on Computers, 408 - 415.

Pegoraro, R.J., 1994, *Texture Analysis in Mountain and Urban Land Use Classifications* : M.sc. Thesis, Department of Geomatics, University of Calgary.

Weszka, J.S., Dyer, C.S. and Rosenfeld, A.,1976, *A Comparative Study of the Texture Measures for Terrain Classification* : IEEE Transactions on Systems, Man , and Cybernetics, SMC-6.

FURTHER READING

Gurney, C.M., 1981, *The Use of Contextual Information in the Classification of Remotely Sensed Data* : International Journal of Remote sensing, 2, 378-388.

Caelli, T.M., 1988 *An Adaptive Computational Model For Texture Segmentation* : IEEE Transactions on Systems, Man, and Cybernetics, 18.

Chittineni, C.B., 1981, *Utilization of Spectral - Spatial Information in the Classification of Imagery Data* : Computer, Graphics, and Image Processing, 16, 305 - 340.

Dutra, L.V. and Mascarkas, C.M., 1984, *Some Experiments with Spatial Feature Extraction Methods in Multispectral Space* : International Journal of Remote Sensing, 5, 303 - 313.

Franklin, S.E. and Peddle, D.R., 1989, *Spectral Texture for Improved Class Descrimination in Complex Terrain* : International Journal of Remote Sensing, 10, 1437-1443.

Franklin, S.E. and Peddle, D.R., 1990, *Classification of SPOT HRV Imagery and Texture Features* : International Journal of Remote Sensing, 11, 551-556.

Franklin, S.E. and Peddle, D.R., 1991, *Image Texture Processing and Data Integration for Surface Pattern Discrimination* : P. E. & R. S., 57, 413-420.

He, D.C.,Wang and L., Guibert, J, 1988, *Texture Descrimination Based on Optimal Utilization of Texture Features* : Pattern Recognition, 21, 141 - 146.

Kashyap, R.L., Chellapa, R. and Khatanzd, A., 1982, *Texture Classification Using Features Derived From Random Field Models* : Pattern Recognition Letters 1, 43 - 50.

Roan, S.J., Aggarwal, J.K. and Martin, W.N., 1983, *Multiple Resolution Imagery and Texture Analysis* : Pattern Recognition, 20, 17-31.

Robinson, E.A. and Treitel, S., 1980, *Geophysical Signal Analysis* : Prentice-Hall, Englewood Cliffs, N.J.

Wong, A.K.C. and Vogel, M.A., 1977, *Resolution Dependent Information Measures for Image Analysis* : IEEE Transactions on Systems, Man, and Cybernetics, SMC-7.